Sudestada1, a *Drosophila* ribosomal prolyl-hydroxylase required for mRNA translation, cell homeostasis, and organ growth

Maximiliano J. Katz[a,b,1], Julieta M. Acevedo[a,b,1], Christoph Loenarz[c], Diego Galagovsky[a,b], Phebee Liu-Yi[d], Marcelo Pérez-Pepe[a,b], Armin Thalhammer[c], Rok Sekirnik[c], Wei Ge[c], Mariana Melani[a,b], María G. Thomas[a,b], Sergio Simonetta[a,b], Graciela L. Boccaccio[a,b,e], Christopher J. Schofield[c], Matthew E. Cockman[d], Peter J. Ratcliffe[d], and Pablo Wappner[a,b,e,2]

[a]Fundación Instituto Leloir, C1405BWE Buenos Aires, Argentina; [b]Consejo Nacional de Investigaciones Científicas y Técnicas, C1405BWE Buenos Aires, Argentina; [c]Chemistry Research Laboratory and Oxford Centre for Integrative Systems Biology, University of Oxford, Oxford OX1 3TA, United Kingdom; [d]Centre for Cellular and Molecular Physiology, University of Oxford, Oxford OX3 7BN, United Kingdom; and [e]Departamento de Fisiología, Biología Molecular y Celular, Facultad de Ciencias Exactas y Naturales, Universidad de Buenos Aires, 1428 Buenos Aires, Argentina

Genome sequences predict the presence of many 2-oxoglutarate (2OG)-dependent oxygenases of unknown biochemical and biological functions in *Drosophila*. Ribosomal protein hydroxylation is emerging as an important 2OG oxygenase catalyzed pathway, but its biological functions are unclear. We report investigations on the function of Sudestada1 (Sud1), a *Drosophila* ribosomal oxygenase. As with its human and yeast homologs, OGFOD1 and Tpa1p, respectively, we identified Sud1 to catalyze prolyl-hydroxylation of the small ribosomal subunit protein RPS23. Like OGFOD1, Sud1 catalyzes a single prolyl-hydroxylation of RPS23 in contrast to yeast Tpa1p, where Pro-64 dihydroxylation is observed. RNAi-mediated Sud1 knockdown hinders normal growth in different *Drosophila* tissues. Growth impairment originates from both reduction of cell size and diminution of the number of cells and correlates with impaired translation efficiency and activation of the unfolded protein response in the endoplasmic reticulum. This is accompanied by phosphorylation of eIF2α and concomitant formation of stress granules, as well as promotion of autophagy and apoptosis. These observations, together with those on enzyme homologs described in the companion articles, reveal conserved biochemical and biological roles for a widely distributed ribosomal oxygenase.

fruit fly | ribosome | dioxygenase | proline | tranlational stress

Iron [Fe(II)]- and 2-oxoglutarate (2OG)-dependent oxygenases are a superfamily with diverse biochemical and biological functions. During 2OG oxygenase catalysis, substrate oxidation is coupled to decarboxylation of 2OG, yielding succinate and carbon dioxide (1, 2). Structural studies reveal that the catalytic domain of 2OG oxygenases contains a conserved double-stranded β-helix (DSBH) fold presenting an HXD...H facial triad motif that coordinates an Fe(II) cofactor (3, 4). These and other structural features have been used to predict the existence of multiple uncharacterized 2OG oxygenases. In contrast to microorganisms and plants where 2OG oxygenases catalyze a wide variety of oxidative reactions, in animals their biochemical activities appear limited to hydroxylations or demethylations via hydroxylation (1, 5, 6). Despite progress in making biochemical assignments, the physiological roles of most 2OG oxygenases predicted by bioinformatic analysis of animal genomes are unknown. For instance, we have identified ~50 putative 2OG oxygenases in the *Drosophila* genome, but only a few are characterized (7, 8).

The function of Fatiga, the single *Drosophila* homolog of human hypoxia inducible transcription factor (HIF) prolyl-4-hydroxylases (PHDs), has been well studied in the context of oxygen sensing (9). HIF prolyl-hydroxylation plays a central role in the animal hypoxic response via hydroxylation of HIF, a posttranslational modification that signals for HIF-α degradation in a physiologically relevant

oxygen-dependent manner (10, 11). Given the tractability of these enzymes as targets for pharmacological modulation by 2OG analogs and related compounds, elucidation of the function of related 2OG oxygenases in biology is an area of current interest (12, 13).

To identify other oxygenase-catalyzed reactions with signaling roles, we have conducted an RNAi-based screen of 2OG oxygenases for phenotypes in *Drosophila*. We identified CG44254, a highly conserved gene that is distantly related to oxygen sensing PHDs (14), as necessary for normal growth and mRNA translation in the fly. This gene, which we have termed *sudestada1* (*sud1*) after a wind that blows across the southeastern coast of South America, is highly conserved from yeast to humans; homologous genes in *Saccharomyces cerevisiae* (*TPA1*) (15, 16), *Schizosaccharomyces pombe* (*Ofd1*) (17, 18), and *Homo sapiens* (*OGFOD1*) (19, 20) have been implicated in translation termination, oxygen-dependent regulation of the transcription factor Sre1N, and translational stresses responses, respectively.

In independent work, reported in companion articles, we discovered that Tpa1p, Ofd1, and OGFOD1 are protein hydroxylases

Significance

Emerging evidence indicates that posttranslational hydroxylation of intracellularly localized proteins is more prevalent than once thought. We identify *Drosophila melanogaster sudestada1 (sud1)* as a gene that is needed for normal growth in the fly and show that *sud1* encodes a prolyl-hydroxylase that catalyzes posttranslational hydroxylation of a conserved residue in the small ribosomal subunit protein RPS23. Knockdown of Sud1 results in growth impairment and reduced RPS23 hydroxylation, which is associated with activation of the unfolded protein response, induction of apoptosis, and increased autophagy. Together with findings in humans and yeast reported in the companion articles, the work reveals a new type of posttranslational ribosome modification that is highly conserved in eukaryotes.

that catalyze unique di- and monohydroxylations of a conserved prolyl residue in the small ribosomal subunit protein RPS23 (21, 22). Here we describe the biochemical and physiological characterization of Sud1 in *Drosophila melanogaster*. We show that Sud1 is a dioxygenase that catalyses monohydroxylation of RPS23 in the fly and that its silencing results in growth defects and impairment of mRNA translation, along with the induction of Eukaryotic Initiation Factor 2α (eIF2α) phosphorylation, stress granule formation, autophagy and apoptosis.

Results

Sudestada1 Encodes the *Drosophila* Tpa1p/OGFOD1 Homolog and Is Required for Normal Growth.

In initial studies, we carried out an RNAi screen in *Drosophila* to identify 2OG oxygenases that lead to impaired growth after knockdown (Table S1). These studies led to the identification of a potential *Ofd1/TPA1/OGFOD1* homolog (CG44254) that we name *sudestada1* (*sud1*). Two transcripts generated by alternative splicing, *sud1* and *sud2*, are reported in databases that curate high-throughput transcriptomic data (http://flybase.org) (Fig. S1*A*). RT-PCR analyses confirm the expression of both transcripts in larvae (Fig. S1 *B* and *C*). Only Sud1 includes a predicted oxygenase domain encompassing residues 171–275 that manifests a substantial degree of identity with Tpa1p/Ofd1/OGFOD1 (Fig. S1 *D* and *E*). Sud2 encodes a predicted phosphatidylinositol-glycan biosynthesis class S protein that is apparently unrelated to oxygenases and has not been investigated in this work.

We then analyzed the mRNA expression profile of *sud1* through the fly life cycle. Quantitative real-time RT-PCR (qRT-PCR) assays reveal *sud1* mRNA expression at all developmental stages, with the highest levels at the first larval instar (Fig. 1*A*). We then compared expression in third-instar larval tissues and found that *sud1* mRNA is highly expressed in the fat body, with significant expression in other organs including the brain, salivary glands, imaginal discs, and gut (Fig. 1*B*). To study the subcellular localization of Sud1, we generated a Sud1-GFP fusion construct and expressed this using the Gal4-UAS system in different tissues (Fig. 1 *C–H*); Sud1 localizes predominantly to the nucleus, although lower levels are also detected in the cytoplasm.

To investigate Sud1 functions, we first expressed a double-stranded RNA that specifically targets *sud1* sequences, without affecting *sud2* mRNA levels (Fig. S1 *B* and *C*). Given that *S. cerevisiae* Tpa1p and *S. pombe* Ofd1 have putative active sites in the *N*-terminal of their two DSBH domains that possess similarity to PHD2 (15, 23), we tested whether Sud1 plays a role in the HIF-dependent transcriptional response to hypoxia by observing the effects of Sud1 knockdown on HIF/Sima-dependent transcription in the embryonic tracheal system. Embryos expressing

sud1 RNAi failed to modulate a HIF-dependent transcriptional reporter, whereas, as expected, embryos that express an RNAi targeting the prolyl-4-hydroxylase gene *fatiga* displayed strong up-regulation of the same reporter under mild hypoxic conditions, providing a positive control for the assay (Fig. S2 *A–D*).

Ubiquitous *sud1* RNAi expression mediated by an *actin*-Gal4 driver was lethal at the second larval instar. To enable phenotypic analysis of the effect of Sud1 suppression at later developmental stages, we used more restricted RNAi interventions. Because Sud1 is most expressed in the fat body, we expressed *sud1* RNAi in this organ, using the driver *pumpless*-Gal4 (*ppl*-Gal4). Restricted silencing allowed development of viable adults. Analysis of the fat body of third-instar larvae of such flies revealed a significant reduction of cell size (Fig. 2 *A–C*). Because reduction of fat body size can have a systemic effect on body growth (24, 25), we measured pupal size and observed a significant reduction in the volume of individuals expressing *sud1* RNAi in the fat body (Fig. 2 *D* and *E*). To determine whether Sud1 suppression impairs growth in other fly organs, *sud1* RNAi was expressed in the wing imaginal disc. In both the posterior (Fig. 2 *F–H*) and the dorsal (Fig. S2 *E* and *F*) compartments of the disc, *sud1* RNAi significantly reduced growth. To verify that the effect of the RNAi is due to Sud1 silencing, the homologous *Drosophila willistoni sud1* gene was coexpressed and found to restore the growth defect (Fig. 2*H*). To test whether Sud1 function is conserved across species, we coexpressed human *OGFOD1*, together with *sud1* RNAi, in the wing posterior compartment. Although incomplete, we again observed restoration of the growth that had been reduced by Sud1 silencing (Fig. 2*H*), implying that the mammalian and fly dioxygenases are functionally conserved.

We next studied effects on cell size. Because all epidermal cells of the *Drosophila* wing produce a single cuticular hair, hair density was used to assess cell density and hence to calculate both cell size and cell number in the wing posterior compartment. In comparison with control RNAi, *engrailed*-Gal4–driven expression of *sud1* RNAi induced an increase in cell density (Fig. 2 *I–K*), indicating that the 21% reduction of the wing posterior compartment (Fig. 2*K*) arose from both a reduction in cell size (15%) and a reduction in cell number (6%).

Sudestada1 Hydroxylates the Ribosomal Protein RPS23.

It is known that mutations in ribosomal proteins can provoke growth defects in *Drosophila*, such as those observed after Sud1 knockdown (26, 27). Consistent with this, in refs. 21 and 22, it is shown that the Sud1 homologs in humans and yeast catalyze a posttranslational modification of a protein of the small ribosomal subunit termed RPS23. Whereas human OGFOD1 mediates monohydroxylation of proline 62 of RPS23, yeast Tpa1p/Ofd1 and its green algae homolog catalyze dihydroxylation of the analogous prolyl residue.
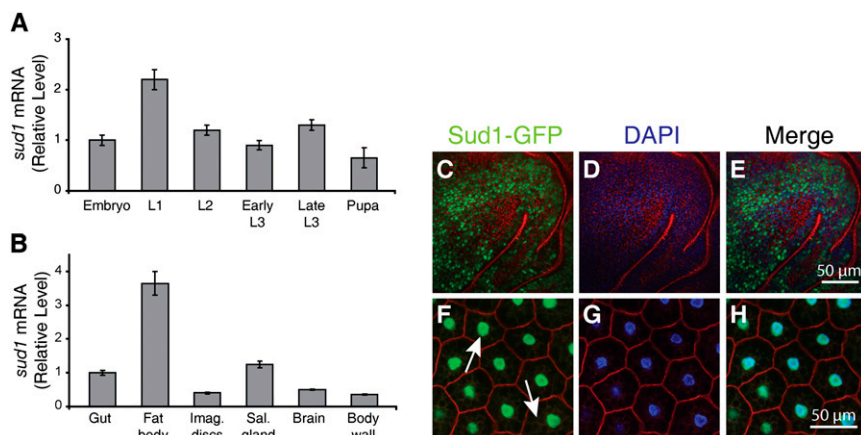

Fig. 1. Expression and subcellular localization of *sudestada*1. (*A*) Temporal *sud1* expression pattern throughout the fly life cycle, as determined by real-time RT-PCR (qRT-PCR); error bars represent SD. (*B*) Expression of *sud1* mRNA in different organs of third-instar larvae. (*C–H*) Expression of a UAS-Sud1-GFP fusion construct in wing imaginal discs (*C–E*) or the fat body (*F–H*). In both tissues, the protein is mostly nuclear, although some GFP signal can be seen at the cytoplasm (arrows in *F*).
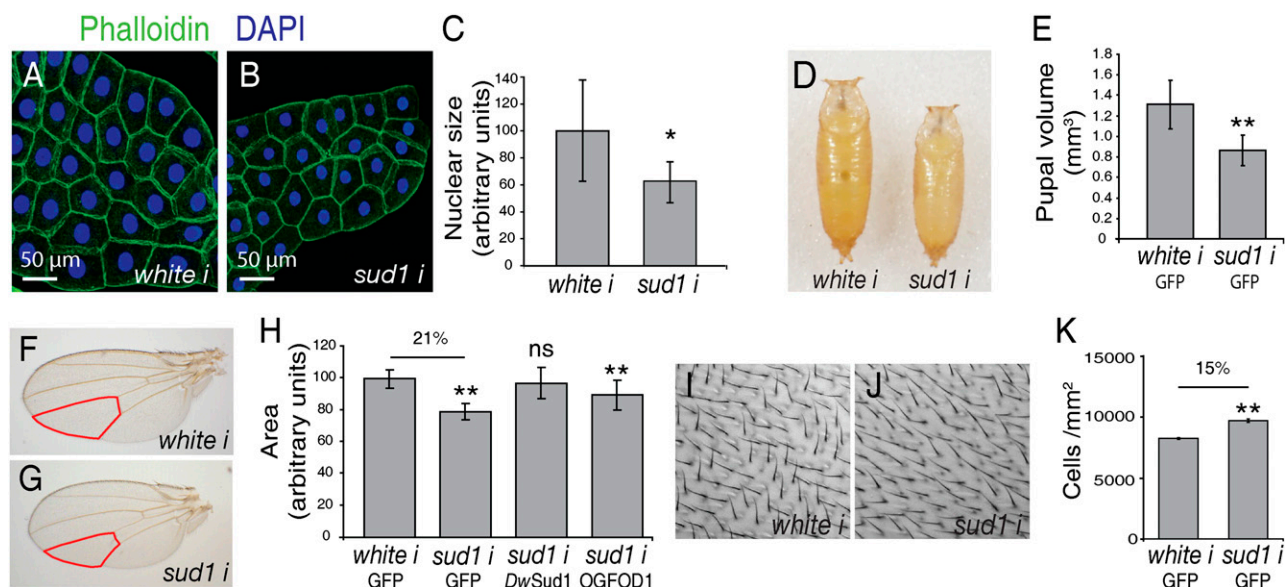
Fig. 2. Sud1 loss of function affects growth. (*A–C*) Sud1 silencing in the fat body of third-instar larvae provokes cell size reduction. *white* (control) (*A*) or *sud1* (*B*) double-stranded RNAs were expressed under control of a *pumpless*-Gal4 (*ppl*-Gal4) driver; fat body cells expressing *sud1* RNAi are smaller than those of the control as assessed by quantification of the area of cell nuclei (*C*). $n = 3$ independent experiments, error bars represent SD, and $*P < 0.01$ (Student t test). (*D* and *E*) As a consequence of *ppl*-Gal4–driven expression of *sud1* RNAi, pupal volume is reduced in comparison with that of a control line expressing a *white* RNAi. $n \geq 25$ in three independent experiments. Error bars represent SD; $**P < 0.001$ (Student t test). (*F–H*) Expression of *sud1* RNAi in the wing disc posterior compartment results in growth impairment: the area limited by wing veins L4, L5, the posterior cross-vein, and the wing margin (marked in red in *F* and *G*) was measured as an indication of the variation of the area of the posterior compartment; (*H*) area quantification after *sud1* RNAi expression, and rescue of the WT wing phenotype after concomitant expression of a *Drosophila willistoni sud1* or human *OGFOD1* transgenes (DwSud1; OGFOD1); the rescue after expression of human OGFOD1 was partial. $n \geq 30$ in three independent experiments. Error bars represent SD ($**P < 0.001$; one-way ANOVA with Tukey post hoc test). (*I–K*) Cell size and cell number are both reduced after expression of *sud1* dsRNA: wing hair density increases after expression of *sud1* RNAi (*K*), indicating that cell size is reduced. Cell size reduction (15%) accounts only partially for reduction of the area of the wing posterior compartment after *sud1* RNAi treatment (21%) (cf. *H* and *K*). The remaining area reduction is due to a decreased number of cells in the compartment (6%). $n \geq 10$ in three independent experiments. Error bars represent SD ($**P < 0.001$; Student t test).

Sequence alignments reveal that the RPS23 prolyl residue that is subject to Tpa1p/OGFOD1-dependent hydroxylation is conserved in *Drosophila* (Fig. 3*A*).

We therefore investigated whether *Drosophila* RPS23 is post-translationally modified. Ribosomes were purified from *Drosophila* Schneider2 (S2) cells grown in culture and then subjected to ultra-performance liquid chromatography (UPLC)-coupled intact protein mass spectrometric analysis. A species corresponding to *Drosophila* RPS23 was observed with a mass +16 Da greater than that predicted from the primary sequence, consistent with addition of a single oxygen atom (Fig. 3*B*). To investigate the dependence of this modification on Sud1, S2 cells were treated with *sud1* RNAi, and LC-MS analyses were performed on Arg-C–digested ribosomal RPS23 preparations. Consistent with the whole-protein MS data (Fig. 3*B*), a peptidic fragment containing Pro-62 was observed with a mass increment of +16 Da. No unmodified species was observed in material prepared from untreated cells, consistent with RPS23 being monohydroxylated. However, after Sud1 silencing, a second species corresponding to the unhydroxylated parent peptide became apparent (Fig. 3 *C* and *D* and Fig. S3 *A* and *B*), indicating that Sud1 is necessary for the hydroxylation. To directly investigate whether Sud1 catalyses RPS23 prolyl hydroxylation, we prepared recombinant RPS23 either alone or coexpressed with Sud1 in a His-tagged form in *Escherichia coli*. A tryptic RPS23 fragment (residues 55–67) revealed a mass shift of +16 Da, which was assigned using MS/MS analyses to Pro-62, implying that Sud1 is the RPS23 prolyl monohydroxylase (Fig. 3*E* and Fig S3 *C–E*). In none of the studies on Sud1/RPS23, either on cellular prepared material or when working with purified protein, did we observe evidence of a +32-Da mass shift corresponding to di-hydroxylation of RPS23 as observed for yeast

Tpa1p/Ofd1 and green algae (*Ostreococcus tauri*) otOGFOD1 (21). Taken together, these experiments indicate that Sud1 catalyzes mono-, but not dihydroxylation of RPS23 Pro-62.

Sudestada1 Knockdown Affects Protein Synthesis and Triggers the Unfolded Protein Response. To further investigate the effects of Sud1 knockdown, we analyzed the effects of *sud1* RNAi on protein synthesis. Wing imaginal discs, ubiquitously expressing either *sud1* or a control dsRNA, were incubated with [^{14}C]-labeled amino acids, and incorporation into protein was measured. A significant decrease of protein synthesis occurred in discs expressing *sud1* RNAi in comparison with controls (Fig. S4 *A* and *B*). Next, we analyzed the phosphorylation status of the translation initiation factor eIF2α, a key regulatory step in the control of cap-dependent mRNA translation. Sud1 silencing in the posterior wing disc compartment promotes substantial increase in P-eIF2α staining that is clearly limited to the posterior wing disc compartment, whereas in flies expressing control RNAi, P-eIF2α was evenly distributed across the whole disc (Fig. 4 *A–D*). This effect was specifically dependent on Sud1 silencing, because coexpression of the *Drosophila willistoni sud1* transgene largely suppressed the induction of P-eIF2α (Fig. S4 *C–F*). This effect of *sud1* RNAi on eIF2α phosphorylation was further confirmed by immunoblotting of extracts prepared from cultured S2 cells after treatment with *sud1* RNAi (Fig. 4*E*). Because eIF2α phosphorylation induces stress granule formation (28), we analyzed for Sud1-linked formation of stress granules. Extensive stress granule formation was observed in S2 cells treated with *sud1* RNAi compared with control RNAi (Fig. 4 *F–I* and Fig. S4 *G* and *H*). Together, these experiments suggest that Sud1 knockdown leads to increased eIF2α phosphorylation, which in turn diminishes protein synthesis and promotes stress granule accumulation.

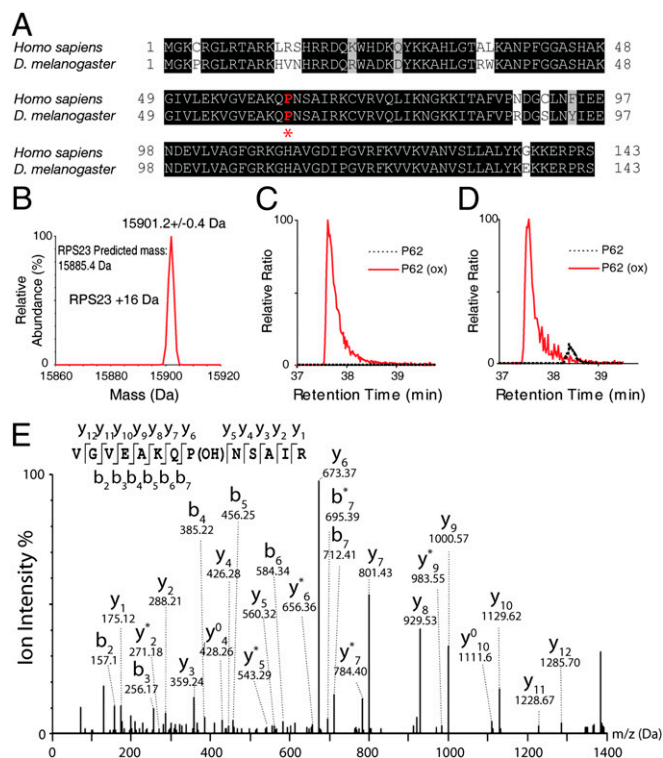Katz et al.

Fig. 3. Sudestada1 hydroxylates RPS23. (*A*) *Drosophila* and human ribosomal protein RPS23 are almost identical. Conserved residues between the two proteins are marked in black; Pro-62 is highlighted in red and marked with an asterisk. (*B*) Deconvoluted ESI-MS whole protein spectrum of *D. melanogaster* RPS23 isolated from S2 cell ribosomes purified by sucrose density sedimentation followed by online UPLC mass spectrometry. A mass of 15,901.2 Da is consistent with a +16-Da shift relative to predicted mass of 15,885.4 Da (*N*-terminal methionine cleaved), indicative of oxidative modification. Note there is no evidence for proline dihydroxylation. (*C* and *D*) Hydroxylation of RPS23 is suppressed by *sud1* dsRNA. Extracted ion chromatograms of *m/z* 670.057 and *m/z* 675.39 corresponding to unhydroxylated (dashed line) and hydroxylated (solid red line) forms of the Pro-62 containing RPS23 peptide GIVLEKVGVEAKQPNSAIR ([M+3H]$^{3+}$) isolated from S2 cells treated with control (*C*) or *sud1* dsRNA (*D*) (see Fig S3 *A* and *B* for assignment of species). (*E*) LC-MS/MS analysis of trypsinized GST-RPS23 after coexpression with Sudestada1. MS/MS spectrum of trypsinized RPS23 after coexpression with His$_6$-Sudestada1 in *E. coli* reveals a peptide, 55-VGVEAKQPNSAIR-67, with a complete series of y-ions demonstrating monohydroxylation (+16 Da) at Pro-62. The b and y fragment ions are indicated (peptide precursor ion: M_r 1,383.760048 Da; calculated 1,383.7470 Da; see Fig. S3*E* for assignment of species).

Because eIF2α phosphorylation is triggered by the unfolded protein response (UPR) (29), among other stimuli, we investigated whether the UPR is triggered by Sud1 knockdown. As a marker of UPR induction, we measured splicing of *xbp1* mRNA, a transcription factor that induces ER chaperones and that is activated by splicing in response to UPR. We used transgenic flies expressing an Xbp1-GFP reporter that generates an in-frame transcript when splicing of the *xbp1* mRNA has occurred (30). This reporter was coexpressed in the wing disc posterior compartment, along with *sud1* RNAi or a control RNAi. As expected, *xbp1* splicing did not occur with expression of the control RNAi (Fig. 4 *J–J'''*), but was strongly induced both by exposure of the discs to DTT (DTT is an established inducer of UPR; Fig. 4 *K–K'''*) and by expression of *sud1* RNAi (Fig. 4 *L–L'''*). Consistent with activation of *xbp1* splicing, ubiquitous expression of *sud1* RNAi at the first larval instar provoked the up-regulation of the endogenous Xbp1 target gene *bip1*, as determined by RT-PCR (Fig. S4*I*). To investigate the extent to which UPR

activation and eIF2α phosphorylation account for Sud1-dependent growth impairment, we studied growth of the wing posterior compartment in flies coexpressing the *sud1* RNAi simultaneously with an RNAi targeting *perk*, the *Drosophila* ortholog of PKR-related ER kinase (PERK). Silencing of PERK partially suppresses the reduction of growth induced by Sud1 knockdown (Fig. 4 *M* and *N*), suggesting that UPR activation accounts, at least in part, for the observed growth impairment.

Sudestada1 Knockdown Triggers Autophagy and Apoptosis. One consequence of UPR activation is induction of autophagy (31). Autophagy affects growth by reducing cell size in various *Drosophila* tissues (32), so we hypothesized that autophagy contributes to the growth impairment observed with Sud1 silencing. Consistent with this, *sud1* RNAi expression in the wing disc posterior compartment provoked induction of autophagy markers in this disc territory, including nucleation of the ATG8-GFP autophagy marker (Fig. 5 *A* and *B*); accumulation of the fluorescent lysosomal probe lysotracker (Fig. 5 *C* and *D*); and formation of large Lamp1-GFP foci (Fig. 5 *E* and *F*). Expression of the *D. willistoni sud1* transgene abolished lysosomal dye accumulation at the posterior disc compartment, again indicating that the action of *sud1* silencing on autophagy is target specific (Fig. S5 *A–C*).

Finally, we investigated whether the reduction in the number of cells observed following expression of *sud1* RNAi (Fig. 2 *I* and *J*) is due to reduced cell proliferation or increased cell death. Phospho-histone3 staining analysis revealed that expression of *sud1* dsRNA in the wing disc posterior compartment does not decrease cell proliferation (Fig. S5*D*), whereas TUNEL staining assays revealed that apoptosis was triggered by *sud1* RNAi (Fig. 5 *G–J*). Reduction of the area of the posterior compartment of the wing following Sud1 silencing was partially suppressed by concomitant expression of the caspase inhibitor p35 (Fig. S5*E*), confirming that induction of apoptosis accounts in part for growth impairment.

Given that the Target of Rapamicin (TOR) pathway plays a central role in growth regulation in the fat body (32), we analyzed genetic interactions between Sud1 and genes of this pathway in this organ. Interestingly, reduction of function of the TOR pathway led to partial suppression of growth defects provoked by Sud1 silencing (Table S2). These results suggest that slowing down translation, as a consequence of TOR down-regulation (33), alleviates the translational stress provoked by Sud1 knockdown.

Discussion

Ribosomal protein hydroxylation mediated by 2OG oxygenases is emerging as an important evolutionary conserved pathway (34). We analyzed the function of Sudestada1, a *Drosophila* oxygenase homolog of human OGFOD1, *S. cerevisiae* Tpa1p, and *S. pombe* Ofd1. We demonstrated that, like OGFOD1, Sud1 mediates hydroxylation of proline 62 of the small ribosomal subunit protein RPS23. Importantly, Sud1 catalyzes a single prolyl hydroxylation, as observed for human OGFOD1 but contrasting with homologs from lower eukaryotes including Tpa1p in yeast, where RPS23 is di-hydroxylated (21). Thus, RPS23 Pro-62 hydroxylation is a unique and highly conserved ribosomal posttranslational modification, but there appears to be a clear biochemical difference between the extent (i.e., mono- or di-) of RPS23 hydroxylation in animals and lower eukaryotes.

Reduction of Sud1 levels causes growth impairment in various *Drosophila* tissues, as observed for OGFOD1 in some human-derived cells (22). The growth defects associated with Sud1 silencing correlated with translational stress, characterized by phosphorylation of eIF2α, the formation of stress granules, induction of UPR, and promotion of autophagy and apoptosis. These findings, along with those on the human and yeast homologs described in the accompanying manuscripts (21, 22), reveal a biochemically

Fig. 4. Sudestada1 knockdown affects protein synthesis and leads to activation of the unfolded protein response. (*A–D*) Phosphorylation of eIF2α is induced at the wing disc posterior compartment after expression of a *sud1* RNAi (*C* and *D*) but not of a *white* RNAi (*A* and *B*), as revealed by anti–P-eIF2α immunofluorescence (red); anti-Engrailed–positive staining identifies the disc posterior compartment (green) (*B* and *D*); DAPI labels cell nuclei (blue). (*E*) Anti–phospho-eIF2α western blot analysis of S2 cell extracts shows that *sud1* but not *gfp* (control) RNAi treatment promotes eIF2α phosphorylation. (*F–I*) Sud1 silencing induces stress granules (SGs) formation. S2 cells treated with a *sud1* RNAi (*G* and *I*) exhibit more stress granules than cells treated with a control *gfp* RNAi (arrow, *F* and *H*), as revealed by polyA FISH. SGs increase after *sud1* silencing occurs both in untreated cells (*F* and *G*) and in cells exposed to sodium arsenite for 2 h (*H* and *I*). (*J–L′″*) *xpb1*splicing is activated after *sud1* knockdown. An Xbp1-GFP splicing reporter was expressed at the disc posterior compartment through an *en*-Gal4 driver, and expression was detected with an anti-GFP antibody; a portion of the disc posterior compartment is shown in *J–L′″*. The reporter is silent in discs expressing a *white* (control) dsRNA (*J*) and is activated after DTT treatment (*K*) or expression of *sud1* RNAi (*L*). In *J′*, *K′*, and *L′*, anti-Engrailed immunostaining confirms the expression of this posterior compartment-specific marker. Wing posterior compartment area (*M*) and cell size (*N*) reduction observed after *sud1* silencing were partially suppressed by concomitant expression of a *perk* double-stranded RNA in the same disc compartment. $n \geq 30$ wings (*M*) and $n = 10$ wings (*N*) in three independent experiments. Error bars represent SD. One-way ANOVA analysis with Tukey comparison (*$*P < 0.05$, **$P < 0.001$).
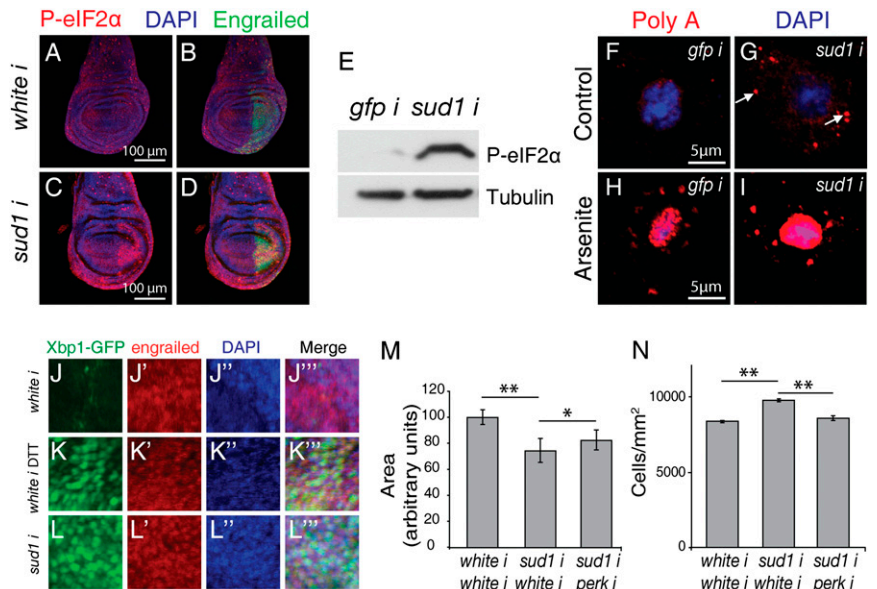
conserved, but context variable, biological role for Sud1/OGFOD1/Tpa1p in the regulation of growth and stress responses.

In flies, Sud1 suppression induces a strong UPR. Furthermore, partial suppression of the growth defects associated with *sud1* RNAi was observed with RNAi directed against *perk*, a key effector kinase in UPR signaling that targets eIF2α (35). Together, these findings suggest that the UPR is at least in part responsible for activation of stress pathways and impairment of growth related to Sud1. The observed induction of autophagy after *sud1*

RNAi expression is also consistent with activation of UPR stress pathways. Despite similar effects on growth, eIF2α phosphorylation, and stress granule formation, induction of the UPR was not observed following OGFOD1 inactivation in mammalian cells (see ref. 22), suggesting the operation of additional signaling systems.

It has recently been reported that OGFOD1 is a stress granule component (20). In contrast with our findings in flies, in that report, OGFOD1 knockdown did not induce stress granule formation, suggesting that induction of translational stress is context determined. We observed suppressive effects of *sud1* RNAi on growth in both the fat body and wing disc compartments together with consistent effects on the induction of stress pathways in both developing flies and cultured *Drosophila* cells. By crossing in loss-of-function alleles of the TOR signaling pathway, and presumably reducing the rate of protein synthesis, growth defects provoked by *sud1* RNAi were partially suppressed, suggesting that translational stress was alleviated. Together with work in mammalian cells described in the accompanying manuscript (22), these results demonstrate that the activation of stress responses by OGFOD1/Sud1 knockdown occur in a number of settings. Nevertheless, as in mammalian and yeast cells, phenotypic responses to Sud1 suppression vary with context. For instance, the growth suppression was affected by nutritional supplementation, as addition of four times the quantity of yeast to the fly medium largely corrected the impairment in wing growth. Together with the effects in mouse embryonic fibroblasts being enhanced by transformation, it is possible that growth restriction by OGFOD1/Sud1 knockdown is enhanced in settings where there is an imbalance between growth and nutrient supply. We have thus far been unable to determine whether this reflects different effects on RPS23 hydroxylation or the downstream integration of signals on stress pathways.

Although there are differences between the effects of Sud1 and OGFOD1 knockdown in respect of the observed activation of the UPR, our results indicate that aspects of both the biochemical function of OGFOD1/Sud1 as ribosomal oxygenases and cellular functions in translational control and stress are conserved. Nevertheless, in other organisms, notably in the
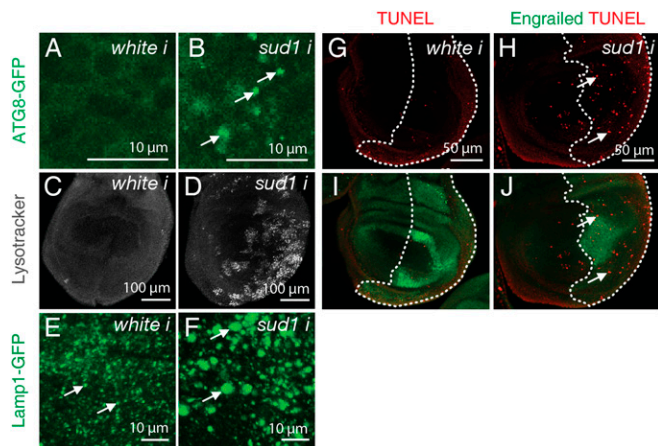
Fig. 5. Autophagy and apoptosis are induced after Sudestada1 knockdown. Expression of a *sud1* (*B*) but not of a *white* (control) (*A*) RNAi at the wing disc posterior compartment provokes nucleation of ATG8-GFP expressed at the same compartment, revealing that autophagy was induced. Autophagy induction was confirmed by Lysotracker-positive staining (*C* and *D*), as well as by nucleation of Lamp1-GFP (*E* and *F*) in cells of the same disc territory. Note in *E* and *F* that small Lamp1-GFP foci become bigger after *sud1* RNAi treatment. (*G–J*) Apoptosis is triggered after *sud1* silencing: Cells of the posterior wing disc compartment expressing *sud1* (*H* and *J*) but not those expressing a *white* (control) RNAi (*G* and *I*) become TUNEL positive (the arrows in *H* show two examples of TUNEL-positive cells). The posterior disc compartment that expresses Engrailed (green staining in *I* and *J*) is marked with a dotted line.

fission yeast *S. pombe*, the homolog Ofd1 has a defined role as an oxygen sensor in the regulation of nuclear transcription by mediating oxygen-dependent proteolysis of Sre1, the homolog of sterol response element-binding proteins (SREBPs) (17, 18). Whether this response is conserved in flies is unclear. However, our analysis reveals that Sud1, like Tpa1p/OGFOD1, is a predominantly nuclear protein. An interesting possibility that will require exploration in future work is whether Sud1 functions in linking ribosomal signals, either generated at preribosomal stages before cytoplasmic export or from the assembled ribosome, to the regulation of nuclear transcriptional responses.

Currently the precise molecular mechanisms linking the growth/stress phenotypes observed in flies to RPS23 hydroxylation are unclear. This relationship is consistent with other studies in which defects in the production or metabolism of protein/nucleic acid components of the ribosome create cellular stress responses (36, 37). As described in refs. 21 and 22, the site of RPS23 hydroxylation is at the ribosomal decoding site and Tpa1p/OGFOD1 affects translation termination efficiency in yeast and mammalian cells.

In preliminary experiments measuring the effects of Sud1 knockdown on stop codon read through using a transgenic bicistronic reporter in *Drosophila*, we observed either no change or small increases in read through at different larval stages, indicating that general increases in stop codon readthrough are unlikely to be the sole Sud1-mediated signal activating the UPR. Nevertheless our results do not exclude the possibility that specific coding errors might be the activating signal, and this is the subject of future investigations.

Materials and Methods

Wing Size Measurement. Wings from 4-d-old females were removed and mounted in a solution containing 1:1 lactic acid/ethanol. Wings were imaged using an Olympus MVX10 stereomicroscope connected to an Olympus DP71 digital camera. The area of the posterior compartment was measured using ImageJ software (National Institutes of Health). To quantify the wing hairs, images were taken using an Olympus BX60 microscope connected to an Olympus DP71 digital camera.

Pupal Size Measurement. Pupae were photographed using the stereomicroscope as previously described. Pupal width and length were measured using Image J software. Volume was estimated using the following formula: $V = \pi D^2(3L - D)/12$, where D is the width and L the length of the pupa.

Fat Body Cell Nuclei Measurement. The area of fat body cell nuclei was measured using the ImageJ Software.

See *SI Materials and Methods* for additional information.

1. Loenarz C, Schofield CJ (2011) Physiological and biochemical aspects of hydroxylations and demethylations catalyzed by human 2-oxoglutarate oxygenases. *Trends Biochem Sci* 36(1):7–18.
2. Ozer A, Bruick RK (2007) Non-heme dioxygenases: Cellular sensors and regulators jelly rolled into one? *Nat Chem Biol* 3(3):144–153.
3. McDonough MA, Loenarz C, Chowdhury R, Clifton IJ, Schofield CJ (2010) Structural studies on human 2-oxoglutarate dependent oxygenases. *Curr Opin Struct Biol* 20(6):659–672.
4. Valegård K, et al. (1998) Structure of a cephalosporin synthase. *Nature* 394(6695):805–809.
5. Tsukada Y (2012) Hydroxylation mediates chromatin demethylation. *J Biochem* 151(3):229–246.
6. Loenarz C, Schofield CJ (2008) Expanding chemical biology of 2-oxoglutarate oxygenases. *Nat Chem Biol* 4(3):152–156.
7. DiTacchio L, et al. (2011) Histone lysine demethylase JARID1a activates CLOCK-BMAL1 and influences the circadian clock. *Science* 333(6051):1881–1885.
8. Herz HM, et al. (2010) The H3K27me3 demethylase dUTX is a suppressor of Notch- and Rb-dependent tumors in Drosophila. *Mol Cell Biol* 30(10):2485–2497.
9. Centanin L, Ratcliffe PJ, Wappner P (2005) Reversion of lethality and growth defects in Fatiga oxygen-sensor mutant flies by loss of hypoxia-inducible factor-alpha/Sima. *EMBO Rep* 6(11):1070–1075.
10. Jaakkola P, et al. (2001) Targeting of HIF-alpha to the von Hippel-Lindau ubiquitylation complex by O2-regulated prolyl hydroxylation. *Science* 292(5516):468–472.
11. Ivan M, et al. (2001) HIFalpha targeted for VHL-mediated destruction by proline hydroxylation: Implications for O2 sensing. *Science* 292(5516):464–468, Epub2001Apr.
12. Mecinović J, Loenarz C, Chowdhury R, Schofield CJ (2009) 2-Oxoglutarate analogue inhibitors of prolyl hydroxylase domain 2. *Bioorg Med Chem Lett* 19(21):6192–6195.
13. Leung IK, et al. (2013) Reporter ligand NMR screening method for 2-oxoglutarate oxygenase inhibitors. *J Med Chem* 56(2):547–555.
14. McDonough MA, et al. (2006) Cellular oxygen sensing: Crystal structure of hypoxia-inducible factor prolyl hydroxylase (PHD2). *Proc Natl Acad Sci USA* 103(26):9814–9819.
15. Henri J, et al. (2010) Structural and functional insights into Saccharomyces cerevisiae Tpa1, a putative prolylhydroxylase influencing translation termination and transcription. *J Biol Chem* 285(40):30767–30778.
16. Keeling KM, Salas-Marco J, Osherovich LZ, Bedwell DM (2006) Tpa1p is part of an mRNP complex that influences translation termination, mRNA deadenylation, and mRNA turnover in Saccharomyces cerevisiae. *Mol Cell Biol* 26(14):5237–5248.
17. Hughes BT, Espenshade PJ (2008) Oxygen-regulated degradation of fission yeast SREBP by Ofd1, a prolyl hydroxylase family member. *EMBO J* 27(10):1491–1501.
18. Lee CY, Yeh TL, Hughes BT, Espenshade PJ (2011) Regulation of the Sre1 hypoxic transcription factor by oxygen-dependent control of DNA binding. *Mol Cell* 44(2):225–234.
19. Saito K, Adachi N, Koyama H, Matsushita M (2010) OGFOD1, a member of the 2-oxoglutarate and iron dependent dioxygenase family, functions in ischemic signaling. *FEBS Lett* 584(15):3340–3347.
20. Wehner KA, Schütz S, Sarnow P (2010) OGFOD1, a novel modulator of eukaryotic translation initiation factor 2alpha phosphorylation and the cellular response to stress. *Mol Cell Biol* 30(8):2006–2016.
21. Loenarz C, et al. (2014) Hydroxylation of the eukaryotic ribosomal decoding center affects translational accuracy. *Proc Natl Acad Sci USA* 111:4019–4024.
22. Singleton RS, et al. (2014) OGFOD1 catalyses prolyl hydroxylation of RPS23 and is involved in translation control and stress granule formation. *Proc Natl Acad Sci USA* 111:4031–4036.
23. Kim HS, et al. (2010) Crystal structure of Tpa1 from Saccharomyces cerevisiae, a component of the messenger ribonucleoprotein complex. *Nucleic Acids Res* 38(6):2099–2110.
24. Delanoue R, Slaidina M, Léopold P (2010) The steroid hormone ecdysone controls systemic growth by repressing dMyc function in Drosophila fat cells. *Dev Cell* 18(6):1012–1021.
25. Colombani J, et al. (2003) A nutrient sensor mechanism controls Drosophila growth. *Cell* 114(6):739–749.
26. Lambertsson A (1998) The minute genes in Drosophila and their molecular functions. *Adv Genet* 38:69–134.
27. Lin JI, et al. (2011) Drosophila ribosomal protein mutants control tissue growth non-autonomously via effects on the prothoracic gland and ecdysone. *PLoS Genet* 7(12):e1002408.
28. Farny NG, Kedersha NL, Silver PA (2009) Metazoan stress granule assembly is mediated by P-eIF2alpha-dependent and -independent mechanisms. *RNA* 15(10):1814–1821.
29. Hetz C (2012) The unfolded protein response: Controlling cell fate decisions under ER stress and beyond. *Nat Rev Mol Cell Biol* 13(2):89–102.
30. Ryoo HD, Domingos PM, Kang MJ, Steller H (2007) Unfolded protein response in a Drosophila model for retinal degeneration. *EMBO J* 26(1):242–252.
31. Kroemer G, Mariño G, Levine B (2010) Autophagy and the integrated stress response. *Mol Cell* 40(2):280–293.
32. Scott RC, Juhász G, Neufeld TP (2007) Direct induction of autophagy by Atg1 inhibits cell growth and induces apoptotic cell death. *Curr Biol* 17(1):1–11.
33. Wullschleger S, Loewith R, Hall MN (2006) TOR signaling in growth and metabolism. *Cell* 124(3):471–484.
34. Ge W, et al. (2012) Oxygenase-catalyzed ribosome hydroxylation occurs in prokaryotes and humans. *Nat Chem Biol* 8(12):960–962.
35. Pomar N, et al. (2003) Functional characterization of Drosophila melanogaster PERK eukaryotic initiation factor 2alpha (eIF2alpha) kinase. *Eur J Biochem* 270(2):293–306.
36. Boglev Y, et al. (2013) Autophagy induction is a Tor- and Tp53-independent cell survival response in a zebrafish model of disrupted ribosome biogenesis. *PLoS Genet* 9(2):e1003279.
37. Danilova N, Sakamoto KM, Lin S (2008) Ribosomal protein S19 deficiency in zebrafish leads to developmental abnormalities and defective erythropoiesis through activation of p53 protein family. *Blood* 112(13):5228–5237.